Title

Rbm24, a target of p53, is necessary for proper expression of p53 and heart development



Journal

Cell Death & Differentiation, 25(6)

ISSN

1350-9047

Authors

Zhang, Min

Zhang, Yanhong

Xu, Enshun

et al.

Publication Date

2018-06-01

DOI

10.1038/s41418-017-0029-8

Peer reviewed

Cell Death & Differentiation (2018) 25:1118–1130
https://doi.org/10.1038/s41418-017-0029-8

Cell Death & Differentiation

ARTICLE

# Rbm24, a target of p53, is necessary for proper expression of p53 and heart development

Min Zhang[1,2] · Yanhong Zhang[1] · Enshun Xu[1] · Shakur Mohibi[1] · Danielle Michelle de Anda[1] · Yuqian Jiang[1] · Jin Zhang[1] · Xinbin Chen[1]

Received: 9 May 2017 / Revised: 29 September 2017 / Accepted: 19 October 2017 / Published online: 22 January 2018


## Abstract

Activation of p53-dependent apoptosis is critical for tumor suppression but aberrant activation of p53 also leads to developmental defects and heart failure. Here, we found that Rbm24 RNA-binding protein, a target of p53, regulates p53 mRNA translation. Mechanistically, we found that through binding to p53 mRNA and interaction with translation initiation factor eIF4E, Rbm24 prevents eIF4E from binding to p53 mRNA and inhibits the assembly of translation initiation complex. Importantly, we showed that mice deficient in *Rbm24* die in utero due to the endocardial cushion defect in the heart at least in part due to aberrant activation of p53-dependent apoptosis. We also showed that the heart developmental defect in *Rbm24*-null mice can be partially rescued by p53 deficiency through decreased apoptosis in the heart. Together, we postulate that the p53-Rbm24 loop is critical for the heart development and may be explored for mitigating congenital heart diseases and heart failure.

## Introduction

Tumor suppressor p53, when activated in response to stress signals, exerts its pro-survival and antigrowth activities by inducing cell cycle arrest, cellular senescence and apoptosis [1, 2]. A fine balance of these p53 activities is necessary for development and thus, aberrant activation of p53 can lead to embryonic lethality or increased risk of congenital malformations [3]. Indeed, several studies showed that inappropriate p53 activation induces CHARGE-like phenotypes and other developmental abnormalities via increased cell-cycle arrest and/or apoptosis [4–6].

Rbm24 and Rbm38 share a high degree of homology, especially in the RNA-Recognition Motif (RRM), and thus constitute a family of RRM-containing RNA-binding proteins [7]. Both Rbm24 and Rbm38 are targets of the p53 family [7, 8] and bind to AU/U-rich elements in target mRNAs, and regulate gene expression via mRNA stability, including p21 and p63 [7–10]. In addition, Rbm38 in turn regulates p53 expression through mRNA translation [11]. Interestingly, mice deficient in *Rbm38* are prone to premature aging and spontaneous tumors [12].

Rbm24 is found to be preferentially expressed in cardiac and skeletal muscle tissues and required for sarcomere assembly and heart contractility [13, 14]. During the preparation of this manuscript, a study showed that loss of *Rbm24* leads to embryonic lethality due to aberrant alternative splicing of key genes necessary for sarcomere formation and cardiogenesis, such as Naca and Fxr1 [14]. Therefore, we examined whether as a target of p53, Rbm24 may in turn regulate p53 expression and whether p53 plays a role in Rbm24-dependent heart development. Here, we found that Rbm24 is necessary for proper p53 expression via mRNA translation. We also found that mice deficient in *Rbm24* die in utero due to failed endocardial cushion morphogenesis and increased p53-dependent apoptosis in

Edited by M. Oren

Min Zhang and Yanhong Zhang contributed equally to this work.

**Electronic supplementary material** The online version of this article (https://doi.org/10.1038/s41418-017-0029-8) contains supplementary material, which is available to authorized users.

✉ Xinbin Chen
xbchen@ucdavis.edu

[1] Comparative Oncology Laboratory, Schools of Veterinary Medicine and Medicine, University of California at Davis, Davis, CA 95616, USA

[2] College of Life Science and Technology, Huazhong Agricultural University, Wuhan, China

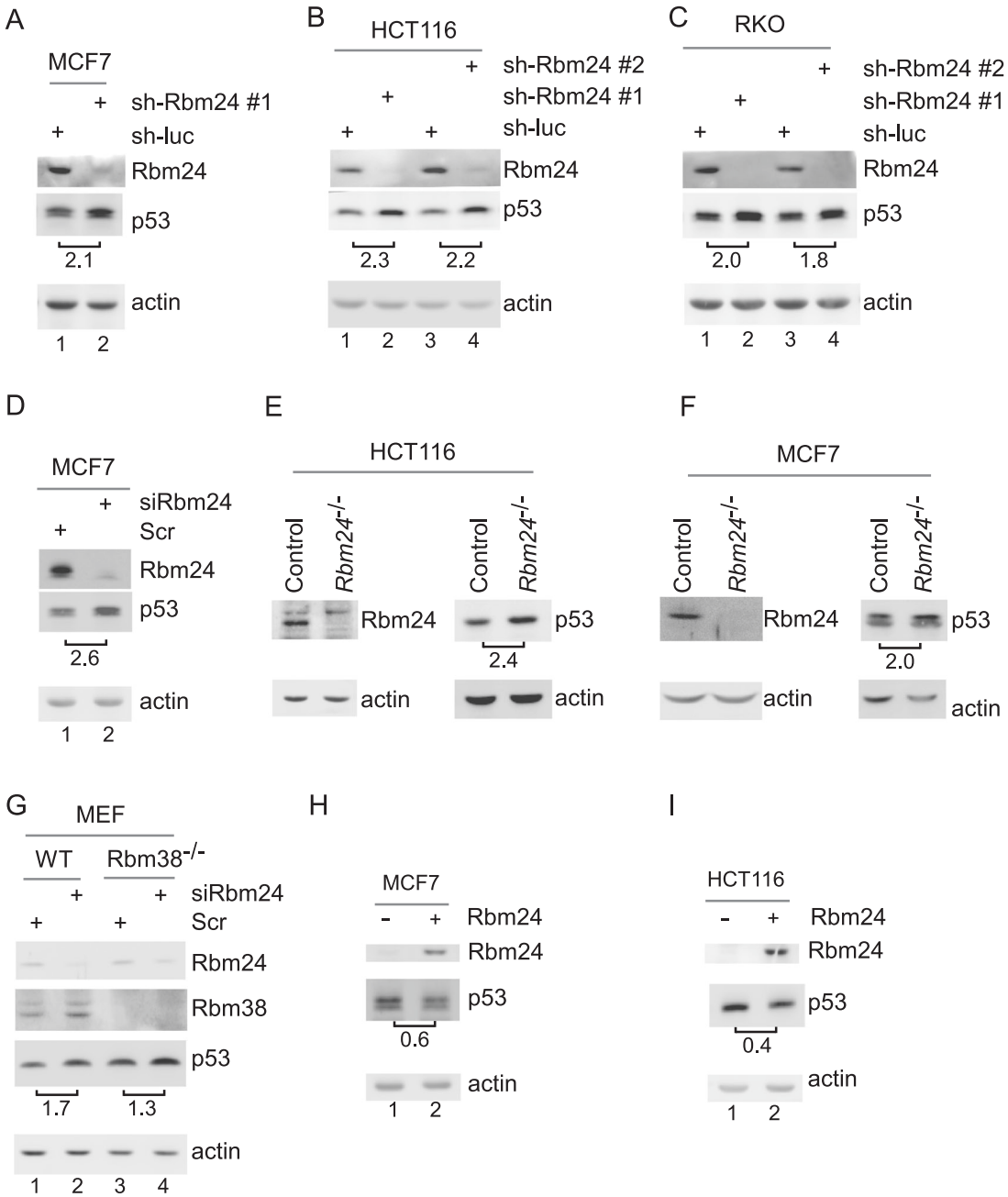


**Fig. 1** Knockdown or knockout of Rbm24 increases, whereas ectopic expression of Rbm24 decreases, the level of p53 protein. **a–c** The levels of Rbm24, p53, and actin proteins were measured in MCF7 (**a**), HCT116 (**b**), and RKO (**c**) cells transduced with a lentiviral vector expressing a control luciferase shRNA (sh-luc) or a Rbm24 shRNA (sh-Rbm24#1 or #2) for 72 h. **d** The levels of Rbm24, p53, and actin were determined in MCF7 cells transiently transfected with scramble siRNA or Rbm24 siRNA for 72 h. **e** The levels of Rbm24, p53, and actin were determined in isogenic control and *Rbm24*-KO HCT116 cells. **f** The experiments were performed as in (**e**) except that isogenic control and *Rbm24*-KO MCF7 cells were used. **g** The levels of Rbm24, p53, and actin were determined in wild-type and *Rbm38*$^{-/-}$ MEFs transiently transfected with scramble siRNA or Rbm24 siRNA for 72 h. **h–i** The levels of Rbm24, p53, and actin were determined in MCF7 (**h**) and HCT116 (**i**) cells uninduced (−) or induced (+) to express Rbm24 for 48 h

cardiac myocytes. Interestingly, the developmental defect in *Rbm24*-null mice can be partially rescued by p53 deficiency, suggesting that aberrant activation of p53 contributes to the phenotypes in *Rbm24*-null embryos. Together, our results suggest that the Rbm24-p53 loop plays a critical role in heart development.

## Results

### P53 expression is regulated by Rbm24 via mRNA translation

Previously, we showed that Rbm24 is regulated by p53 and in turn regulates p21 and p63 expression via mRNA stability [7, 9]. As a homolog of Rbm38 and a target of the p53 family, it is likely that Rbm24 may also regulate p53 expression. To test this, the level of p53 protein was determined in MCF7, HCT116, and RKO cells in which Rbm24 was knocked down by two separate short hairpin RNA (shRNAs) targeting Rbm24 (Figs. 1a–c). We found that upon knockdown of Rbm24, the level of p53 protein was markedly increased (Figs. 1a–c). To confirm this, Rbm24 was knocked down by a small interfering RNA (siRNA) targeting Rbm24 in MCF7 cells. Similarly, the level of p53 was markedly increased upon knockdown of Rbm24 (Fig. 1d). Furthermore, we generated multiple Rbm24 knockout HCT116 and MCF7 cell lines by CRISPR-cas9 and found that the level of p53 protein was much higher in Rbm24-KO cells than that in isogenic control cells (Figs. 1e, f). Since Rbm38 is known to regulate p53 expression, we examined whether the effect of Rbm24 on p53 expression is dependent on Rbm38. We found that, upon knockdown of Rbm24, the level of p53 protein was increased in both wild-type and *Rbm38*$^{-/-}$ MEFs (Fig. 1g), suggesting that Rbm24 regulates p53 expression independent of Rbm38. Conversely, we found that upon ectopic expression of Rbm24 in MCF7 and HCT116 cells, p53 expression was decreased (Figs. 1h, i).

Previously, we found that wild-type Rbm38 and non-phosphorylatable S195A decrease, whereas phosphor-mimetic S195D increases p53 mRNA translation [11]. Since S195 in Rbm38 is conserved as S181 in Rbm24 (Supplementary Fig. S1A), we generated Rbm24-S181D and Rbm24-S181A and then examined whether non-phosphorylatable S181A and phosphor-mimetic S181D have a differential effect on p53 expression. We showed that, like wild-type Rbm24, S181A suppressed p53 expression in both HCT116 and MCF7 cells (Supplementary Fig. S1B). In contrast, S181D increased p53 expression (Supplementary Fig. S1B). These data suggest that, like Rbm38, phosphorylation of S181 would convert Rbm24 from a repressor to an activator of p53 expression if phosphorylated.

Rbm38 is known to repress p53 expression via mRNA translation. To examine whether p53 mRNA translation is regulated by Rbm24, the level of newly synthesized p53 protein was measured in $^{35}$S-labeled HCT116 cells. We showed that the level of newly synthesized p53 protein was decreased by ectopic expression of Rbm24 in HCT116 cells (Fig. 2a). Conversely, we found that the level of newly synthesized p53 protein was highly increased by knockdown of Rbm24 in HCT116 cells (2.9-fold; Fig. 2b) or by knockout of Rbm24 in MCF7 cells (4.2-fold; Fig. 2c). In contrast, the level of p53 transcript was not significantly altered in HCT116 cells in which Rbm24 was knocked down (Fig. 2d).

To confirm the translational repression of p53 by Rbm24, sucrose gradient sedimentation assay was performed to examine the association of polysomes with p53 mRNA in

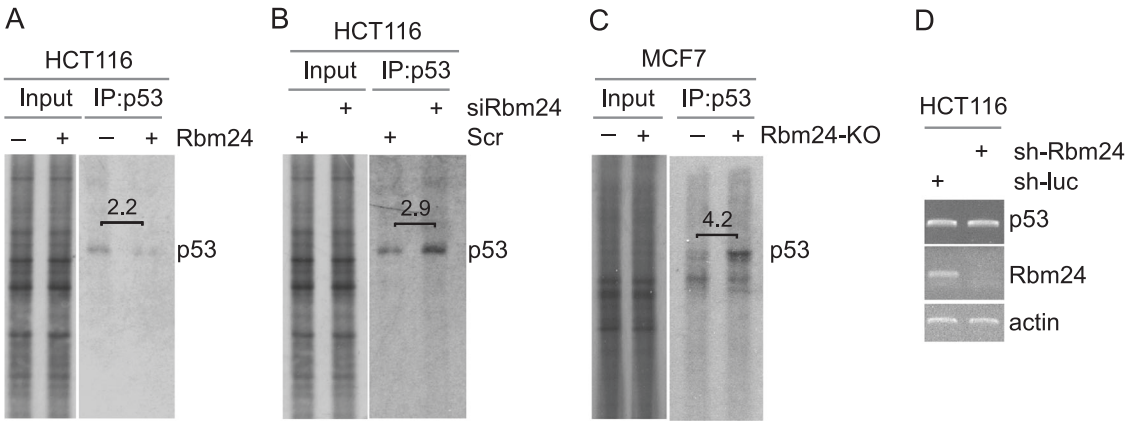


**Fig. 2** Rbm24 regulates p53 expression via mRNA translation. **a** The level of newly synthesized p53 protein is decreased by ectopic expression of Rbm24. HCT116 cells were uninduced or induced to express Rbm24 for 48 h and then $^{35}$S-labeled for 15 min, followed by immunoprecipitation with anti-p53. The immunocomplexes were resolved by SDS-PAGE, and p53 was visualized by autoradiography. **b** The level of newly synthesized p53 protein is increased by knockdown of Rbm24 in HCT116 cells. The experiment was performed as in (**a**) except that HCT116 cells were transiently transfected with scramble siRNA or Rbm24 siRNA for 72 h. **c** The level of newly synthesized p53 protein is increased by knockout of *Rbm24* in MCF7 cells. Isogenic control and *Rbm24*-KO MCF7 cells were $^{35}$S-labeled for 15 min, followed by immunoprecipitation with anti-p53. **d** The levels of Rbm24, p53, and actin transcripts were measured in HCT116 transduced with a lentiviral expressing a control luciferase shRNA (sh-luc) or Rbm24 shRNA (sh-Rbm24) for 72 h

HCT116 cells with or without Rbm24 expression. We showed that the extent of heavy polysomes associated with p53 mRNA, but not with actin mRNA, was significantly decreased upon ectopic expression of Rbm24 (Supplementary Fig. S2).

As a RNA-binding protein, Rbm24 may regulate p53 expression by binding to p53 transcript. To test this, RNA immunoprecipitation assay followed by RT-PCR (RNA-ChIP) was performed using extracts from MCF7 cells (Fig. 3a, right panel) as well as from HCT116 cells that

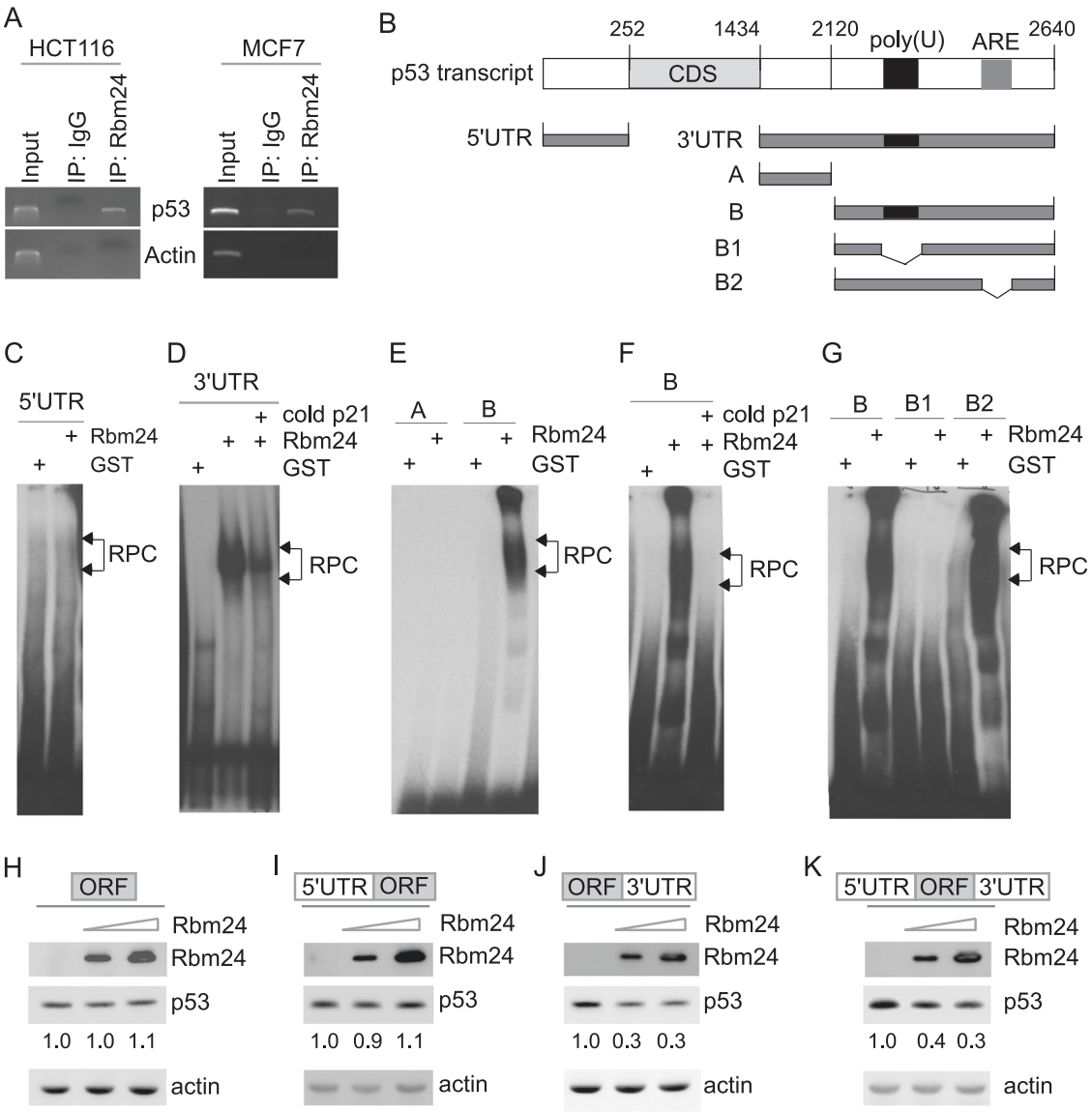


**Fig. 3** The U-rich element in p53 3′UTR is recognized by and responsible for Rbm24 to regulate p53 expression. **a** Rbm24 interacts with p53 transcript. Cell extracts were purified from Rbm24-expressing HCT116 cells (left panel) or MCF7 cells (right panel) and then immunoprecipitated with a control IgG or anti-Rbm24 antibody. The levels of p53 and actin transcripts in Rbm24 or IgG immunocomplexes were determined by RT-PCR. **b** Schematic presentation of p53 transcript and the location of probes used for REMSA. **c**, **d** p53 3′UTR is recognized by Rbm24. REMSA was performed by mixing $^{32}$P-labeled 5′ UTR (**c**) or 3′UTR (**d**) with recombinant GST or GST-Rbm24 protein. The bracket indicates RNA–protein complexes (RPC). Competition assay was performed by adding an excess amount (50-fold) of unlabeled p21 3′UTR to thereaction mix prior to incubation with the $^{32}$P-labeled p53 3′ UTR probe (**d**). **e** REMSA was performed as in (**c**) except that $^{32}$P-labeled probe A or B was used. **f** Competition assay was performed by adding an excess amount (50-fold) of unlabeled p21 3′UTR to the reaction mix prior to incubation with the $^{32}$P-labeled probe B. **g** REMSA was performed as in (**c**) except that probe B, B1, or B2 was used. **h–k** p53 3′UTR is sufficient for Rbm24 to regulate p53 expression. The levels of p53, Rbm24, and actin were measured in H1299 cells, which were co-transfected with a vector expressing Rbm24 along with a vector that contains the p53 coding region (ORF) alone (**h**), p53 ORF plus p53 5′ UTR (**i**), p53 ORF plus p53 3′ UTR (**j**), or p53 ORF plus p53 5′ and 3′ UTRs (**k**). The relative fold change for p53 protein was shown below each lane

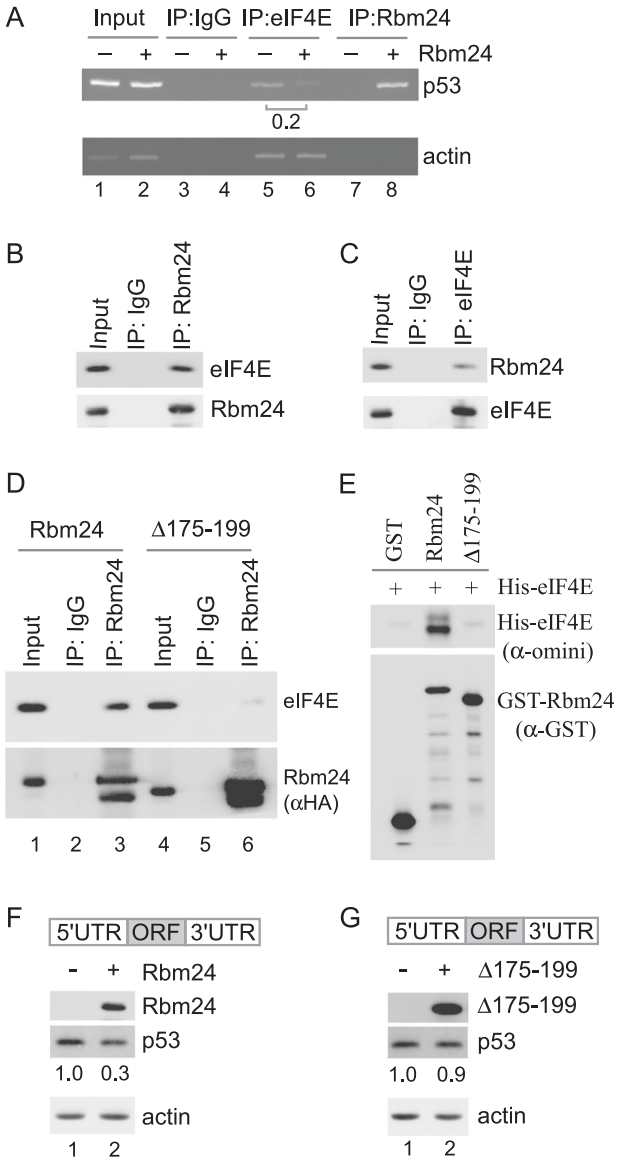


**Fig. 4** Rbm24 interacts with and then prevents eIF4E from binding p53 mRNA. **a** HCT116 cells were uninduced or induced to express HA-tagged Rbm24 for 48 h, followed by immunoprecipitation with control IgG, anti-eIF4E, or anti-HA that recognizes HA-Rbm24. Total RNAs were purified from immunocomplexes and subjected to RT-PCR to measure the levels of p53 and actin mRNAs. The relative fold change in the levels of p53 mRNA was shown below lanes 5–6. **b** Lysates pretreated with RNase A were immunoprecipitated with control IgG or anti-Rbm24. The levels of eIF4E and Rbm24 in Rbm24-containing immunocomplexes were examined by western blot analysis with anti-eIF4E and anti-Rbm24, respectively. **c** The experiment was performed as in (**b**) except that anti-eIF4E was used for immunoprecipitation. **d** Lysates were purified from HCT116 cells, which were transfected with a vector expressing HA-tagged Rbm24 or Rbm24(Δ175–199). The lysates were then pretreated with RNase A and immunoprecipitated with control IgG or anti-HA (Rbm24). The immunocomplexes were examined by western blot analysis with antibodies against HA (Rbm24) or eIF4E. **e** GST pull-down assays were performed by mixing GST, GST-Rbm24, or GST-Rbm24 (Δ175–199) with recombinant His-tagged eIF4E. **f** The levels of p53, Rbm24, and actin were measured in H1299 cells, which were co-transfected with a vector expressing Rbm24 and a vector that carries the p53-coding region plus its 5′ and 3′UTRs. The fold change in the levels of p53 protein was shown below the p53 panel. **g** The experiment was performed as in (**f**) except that a vector expressing Rbm24 (Δ175–199) was used

were induced to express Rbm24 (Fig. 3a, left panel). We found that p53 mRNA was detectable in Rbm24 but not control IgG immunocomplexes (Fig. 3a). As a control, actin transcript was not detected in anti-Rbm24 or IgG immunocomplexes (Fig. 3a).

To delineate Rbm24-binding site(s) in p53 transcript, RNA electrophoretic mobility assay (REMSA) was performed with radiolabeled probes derived from p53 5′ and 3′ UTRs (Fig. 3b). We found that recombinant GST-tagged Rbm24 but not GST alone was able to form a complex with 3′UTR but not 5′UTR probe (Figs. 3c, d). The specificity of the binding of Rbm24 to p53 3′UTR was confirmed by a competition assay in which unlabeled p21 3′UTR cold probe was added to the reaction mixture (Fig. 3d, compare lane 1 with 3). The p21 probe is derived from p21 3′UTR and known to bind to RBM24 [7]. To further delineate the Rbm24-binding region(s) within p53 3′UTR, two subfragments within 3′UTR (A and B) were made for REMSA (Fig. 3b). We found that Rbm24 showed a strong binding to probe B, which contains poly(U) and AU-rich (ARE) elements (Fig. 3b), but not to probe A (Fig. 3e). Similarly, the binding of Rbm24 to B probe was abrogated by cold p21 probe (Fig. 3f). In addition, to define whether Poly(U) and ARE elements are necessary for Rbm24 to recognize p53 3′UTR, we generated probe B1, which lacks Poly(U) element, and probe B2, which lacks ARE element (Fig. 3b). We found that Rbm24 was able to bind to probe B2 but not to probe B1 (Fig. 3g), suggesting that, like Rbm38, Rbm24 recognizes p53 3′UTR via the poly(U) element (Fig. 3b).

To explore whether p53 5′ and 3′UTRs are responsible for Rbm24 to regulate p53, four reporter vectors that contain the p53-coding region (ORF) alone or in combination with p53 5′UTR, 3′UTR, or both [11] were used. We showed that Rbm24 inhibited ectopic p53 expression in a dose-dependent manner as long as the p53 expression vector carries p53 3′UTR (Figs. 3h–k).

To identify the Rbm24-binding site in p53 3′UTR, we generated three green fluorescent protein (GFP) reporters that carry GFP open reading frame only, GFP plus p53 3′UTR, or GFP plus p53 3′UTR without the poly(U) element (Supplementary Fig. S3A). We showed that in *Rbm24* $^{-/-}$ HCT116 cells, GFP expression was inhibited by ectopic expression of Rbm24 from a reporter that carries p53 3′UTR but not the one that carries GFP only or GFP plus poly(U)-deleted p53 3′UTR (Supplementary Fig. S3B).

This suggests that poly(U) element is required for Rbm24 binding to p53 mRNA.

Since p53 5′UTR contains an Internal Ribosome Entry Site (IRES) [15, 16], we examined whether Rbm24 plays a role in p53 translation via p53 IRES. To test this, a bicistronic reporter in that Renilla luciferase is under the control of a CMV promoter and Firefly luciferase can only be translated from p53 IRES was generated (Supplementary Fig. S3C) and then co-transfected with Rbm24 into *Rbm24*$^{-/-}$ HCT116 cells. We showed that the Firefly luciferase activity was not significantly altered by Rbm24 (Supplementary Fig. S3D), suggesting that p53 IRES does not play a major role in Rbm24-mediated regulation of p53 translation.

Rbm38 physically interacts with cap-binding protein eIF4E on p53 transcript, which effectively sequesters eIF4E from binding p53 5′-cap and, thus, represses p53 mRNA translation [11]. To test whether Rbm24 regulates p53 mRNA translation through such a mechanism, RNA-ChIP assay was performed and showed that the level of p53 transcript was highly enriched in Rbm24-containing immunoprecipitates (Fig. 4a, compare lanes 7–8), consistent with the above study (Fig. 3a). Interestingly, upon expression of Rbm24, the level of eIF4E associated with p53 transcript, but not with actin transcript, was markedly decreased (0.2-fold; Fig. 4a, compare lanes 5–6). To determine whether an interaction between Rbm24 and eIF4E is needed to suppress the binding of eIF4E to p53 transcript, IP-WB was performed and showed that eIF4E was detected in anti-Rbm24 immunocomplexes (Fig. 4b). Conversely, we found that Rbm24 was detected in anti-eIF4E immunocomplexes (Fig. 4c).

Previously, we showed that the region from amino acids 189–204 in Rbm38 is necessary for interacting with eIF4E. Thus, we examined whether the region from aa 175–199 in Rbm24, which shares high similarity with the eIF4E-binding site (aa189–204) in Rbm38, is also necessary for interacting with eIF4E. We found that eIF4E formed a complex with wild-type Rbm24 but not mutant Rbm24 (Δ175–199; Fig. 4d). To confirm this, GST-pull down assay was performed and showed that His-tagged eIF4E physically interacted with GST-tagged Rbm24, but not with GST-tagged Rbm24 (Δ175–199; Fig. 4e).

Next, we examined whether the interaction between Rbm24 and eIF4E is required for regulating p53 mRNA translation. To test this, p53 expression was measured in H1299 cells, which were transfected with either wild-type Rbm24 or Rbm24 (Δ175–199) along with a p53 expression vector that contains p53 5′- and 3′UTRs. Consistent with the study above (Fig. 3k), p53 expression was inhibited by Rbm24 (Fig. 4f). In contrast, Rbm24 (Δ175–199) had no effect on p53 expression (Fig. 4g). Thus, we conclude that Rbm24 prevents eIF4E from binding to p53 5′-cap via physical interaction and subsequently suppresses p53 mRNA translation.

## Rbm24 deficiency leads to endocardial cushion defects in developing embryos, which can be partially rescued by deletion of p53

To determine the biological function of Rbm24, we generate *Rbm24*$^{fl/fl}$ mice, which were then crossed with cre transgenic mice (EIIa-cre) to produce *Rbm24*-deficient mice (supplementary Figs. S4A–B). We found that *Rbm24* heterozygous mice developed normally with no gross abnormalities and were fertile. However, no newborn or weaned pups were found with *Rbm24*$^{-/-}$ genotype from 12 litters and 128 mice (supplementary Table S1). These results are consistent with a previous report [14] that Rbm24 is required for embryonic development. We also found that mice deficient in *Rbm24* were grossly normal at E10.5–11.5, but died with growth retardation at E12.5–13.5 and resorption at E14.5 (Figs. 5a, b, Supplemental Fig. S5, and Table S1). To determine the effect of the null mutation on embryogenesis, histological examination was performed on WT and *Rbm24*-null littermate embryos at E10.5 and E11.5 ($n = 4$/time point). We found that all *Rbm24-null* embryos at E10.5 and E11.5 had substantially fewer cells in the atrioventricular cushions compared to WT littermates (Figs. 5a, b). As a result, the atrioventricular endocardial cushions were thinner, and the fusion of the superior and inferior endocardial cushions was inadequate or abnormal, indicating that the endocardial cushion defect leads to defective AV septation and valve development (Figs. 5a, b). E11.5 *Rbm24*-null embryos also exhibited reduced trabeculation (Figs. 5a, b).

Programmed cardiac cell death plays a role in the progression of heart failure, including endocardial cushion defect [17–20]. Since p53 is recognized as a major regulator of cardiac apoptosis [4, 21, 22], we examined whether accumulation of p53 by lack of *Rbm24* leads to aberrant induction of apoptosis and subsequently endocardial cushion defects. To test this, TUNEL assay was performed with E10.5 or E11.5 embryos. A few rare apoptotic cells appeared in the normal WT embryonic heart (Figs. 5c, d), which is consistent with previous reports [23, 24]. In contrast, the number of apoptotic cells in *Rbm24*$^{-/-}$ embryonic heart tissues were significantly higher than that in normal WT embryos (Figs. 5c, d). Consistent with the increased apoptosis, the levels of the p53 protein along with Puma, a p53 target, and a key mediator of p53-dependent apoptosis [25–27] were much higher in *Rbm24*$^{-/-}$ E11.5 embryo than in WT littermate embryo (Fig. 5e). In line with this, we found that the levels of p53 and Puma were increased in *Rbm24*$^{-/-}$ cells compare to that in isogenic control HCT116 cells (Fig. 5f and Supplemental Fig. S7A). In addition, we

found that Puma was not increased in *Rbm24*$^{-/-}$; *p53*$^{-/-}$HCT116 cells (Supplementary Fig. S7A), suggesting that increased expression of p53 by loss of Rbm24 is primarily responsible for increased expression of Puma. Consistently with these observations, colony formation assay showed that Rbm24 deficiency decreased the number

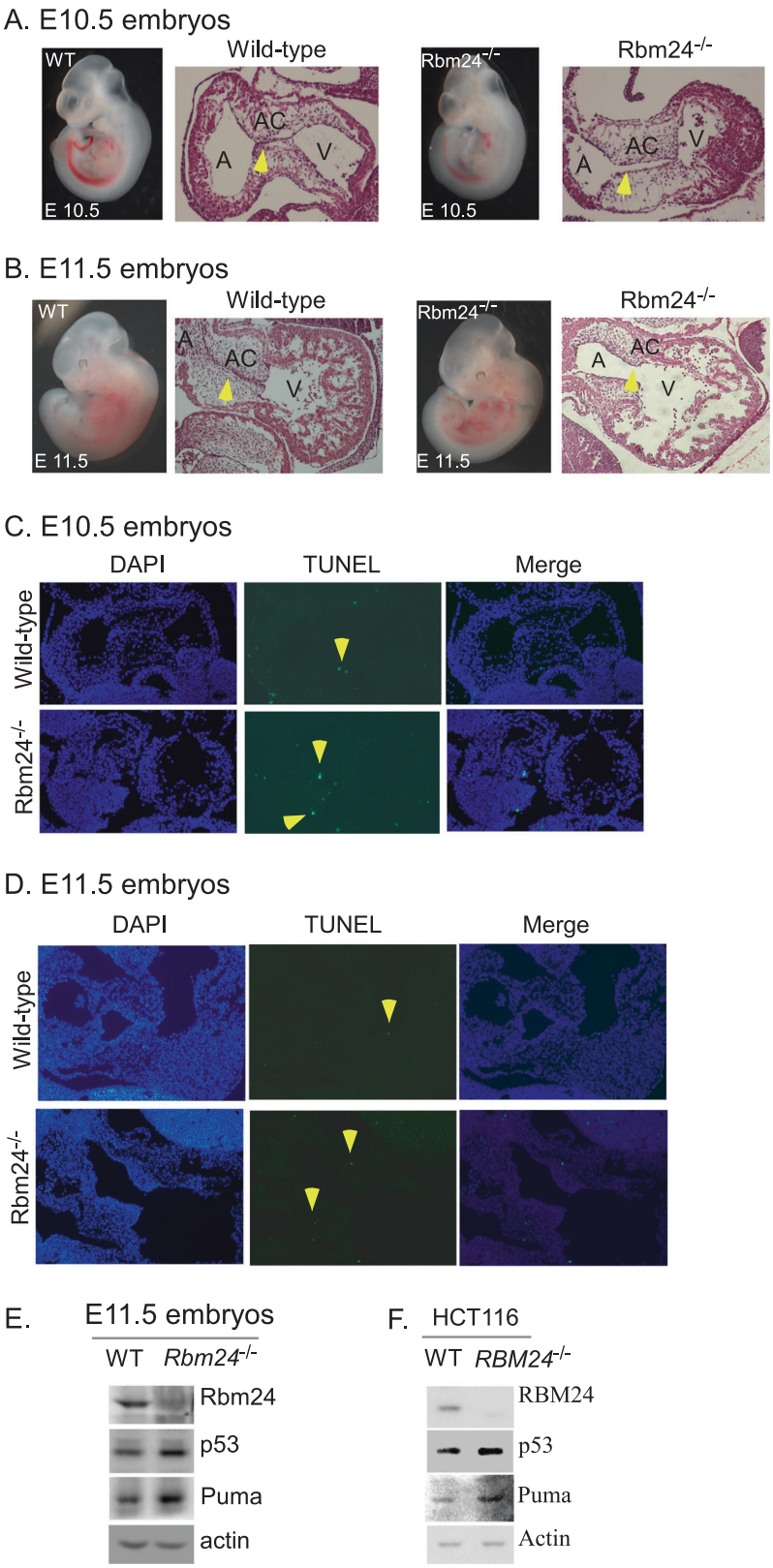


**Fig. 5** Rbm24 is necessary for endocardial cushion development. **a**, **b** Representative images of wild-type and *Rbm24*$^{-/-}$ littermate embryos and H&E-stained sagittal sections of heart at E10.5 (**a**) and E11.5 (**b**). *A* atrium, *AC* atrioventicular cushion, *V* ventricle. **c**, **d** TdT-mediated dUTP nick end labeling (TUNEL) assay was performed with sagittal sections of hearts from wild-type and *Rbm24*$^{-/-}$ embryos at E10.5 (**c**) and E11.5 (**d**). Cell nuclei were stained with 4, 6-diamidino-2-phenylindole (DAPI, blue) and apoptotic bodies were stained in green (FITC). **e** The levels of Rbm24, p53, Puma, and actin proteins in wild-type and *Rbm24*$^{-/-}$ E11.5 embryos were measured by western blot analysis. **f** The experiment was performed as in (**e**) except that isogenic control and *Rbm24*$^{-/-}$ HCT116 cells were used. (Color figure online)

of colonies formed by *Rbm24*$^{-/-}$ HCT116 cells (Supplementary Fig. S7B, left panel). In contrast, Rbm24 deficiency had no effect on the colony-forming capability of *Rbm24*$^{-/-}$;*p53*$^{-/-}$ HCT116 cells (Supplementary Fig. S7B, right panel).

To confirm the role of p53 in the heart development, we tested whether ablation of the *p53* gene can rescue the embryonic lethality in *Rbm24*$^{-/-}$ mice. By intercrossing *Rbm24*$^{+/-}$; *p53*$^{+/-}$ mice, multiple embryos were isolated at E11.5–18.5 (Fig. 6a; Supplementary Figs. S6A–C). We found that unlike *Rbm24*$^{-/-}$ embryos, many *Rbm24*$^{-/-}$; *p53*$^{+/-}$ and *Rbm24*$^{-/-}$; *p53*$^{-/-}$ embryos were viable, some of which exhibited no obvious defect (Fig. 6a; Supplementary Figs. S6A–C). Histological examination was performed and showed that *p53* heterozygosity was sufficient to eliminate the endocardial cushion defects by loss of *Rbm24*$^{-/-}$ in E10.5, E11.5, and E14.5 *Rbm24*$^{-/-}$; *p53*$^{+/-}$ embryos (Figs. 6a–c). We also found that the level of apoptosis increased by loss of *Rbm24* was markedly reduced in *Rbm24*$^{-/-}$; *p53*$^{+/-}$ E11.5 embryos (Fig. 6d). Nevertheless, we would like to note that this rescue was partial since *Rbm24*$^{-/-}$; *p53*$^{+/-}$ embryos still exhibited developmental retardation at E18.5 (Supplementary Fig. S6B).

## Discussion

Here, we found that overexpression of Rbm24 inhibits, whereas knockdown of Rbm24 increases, p53 mRNA translation. Thus, the mutual regulation of p53 and Rbm24 represents a novel feedback loop. We also found that mice deficient in Rbm24 die in utero due to developmental defects in the heart, which can be partially rescued by p53 deficiency. These results suggest that the p53-Rbm24 loop plays a critical role in embryonic development.

During the preparation of this study, Yang et al. reported that mice deficient in Rbm24 display heart developmental failure, resulting in embryonic lethality [14], which is consistent with the finding in this study. Rbm24 is highly expressed in the heart and skeletal muscle [13, 14] and loss of Rbm24 leads to defective endocardial cushion development and subsequently ventricular septal defects (Fig. 5) [14]. As the endocardial cushion is the endocardium-derived structures that build the heart septa and valves [28], endocardial cushion defects would lead to congestive cardiac failure and embryonic lethality.

Studies in human patients and animal models provide compelling evidence that both increased and decreased apoptosis in myocytes would lead to severe congenital heart defects, dilated cardiomyopathy in response to pressure overload, and ischemic heart disease [17, 19–21, 29–33]. In addition, p53-dependent apoptosis in myocytes is considered as a prevailing cause for cardiac dysfunction or remodeling [22, 34–36]. Moreover, attenuation of p53-mediated apoptosis can restore cardiac function in DiGeorge syndrome and myocardial infarction [21, 35, 37]. Here, we showed that like its homolog Rbm38, Rbm24 has emerged as a key molecule to control p53 activity, especially in the heart. We found that loss of Rbm24 stabilizes p53, which induces apoptosis in the heart and subsequently endocardial cushion developmental defect. We also found that embryonic lethality in *Rbm24*-null mice can be partially rescued by loss of p53. Most importantly, *Rbm24*$^{-/-}$; *p53*$^{+/-}$ and *Rbm24*$^{-/-}$; *p53*$^{-/-}$ mice display near-normal development of the endocardial cushion along with reduced apoptosis as compared to *Rbm24*$^{-/-}$ mice. Consistently, PUMA, a target of p53 and an effecter of p53-dependent apoptosis, is induced in *Rbm24*$^{-/-}$ but not WT mouse embryos. Since PUMA is known to play a role in cardiomyocyte apoptosis [38–42], we postulate that aberrant activation of p53-dependent apoptosis accounts for heart developmental defects in *Rbm24*$^{-/-}$ mice.

p53-dependent myocyte apoptosis is a hallmark in the progression of adult heart failure, including dilated cardiomyopathy in response to pressure overload and ischemic heart disease [21, 29, 32, 33]. Here, we showed that the p53-Rbm24 loop plays a role in heart failure. Thus, our study suggests that the p53-Rbm24 loop can be explored to mitigate congenital heart defects and the heart failure in response to chronic pressure overload.

## Experimental procedures

### Reagents

Anti-eIF4E, anti-p53, anti-GST, and anti-histidine were purchased from Santa Cruz Biotechnology (Santa Cruz, CA). Anti-HA was purchased from Covance (San Diego, CA). Anti-actin, proteinase inhibitor cocktail, RNaseA, and protein A/G beads were purchased from Sigma (St. Louis, MO). Anti-Puma was purchased from ProScience (Sapphire Bioscience, Redfern, NSW, Australia). Anti-Rbm24 antibody was made as previously described [7]. The Iscript cDNA synthesis kit was purchased from Bio-Rad Laboratories (Irvine, CA). $^{35}$S-methionine/cysteine and α-$^{32}$P-UTP were purchased from PerkinElmer (Waltham, MA). The Ni-NTA agarose beads were purchased from Biontex (Germany). The glutathione sepharose beads were purchased from Macherey-Nagel (Germany). In Situ Direct DNA fragmentation (TUNEL) assay kit was purchased from Roche (Indianapolis, IN).

### Plasmids

pcDNA3 or pcDNA4 vector expressing Rbm24 or HA-tagged Rbm24 was used as previously described [7].

pcDNA3 vectors expressing Rbm24-S181A or -S181D were generated by two-step PCR reactions (Supplemental Fig. 1A). The primers were listed in Supplementary Table S2. Vectors expressing the p53-coding region (ORF) alone, p53 ORF plus p53 5′UTR, p53 ORF plus p53 3′UTR, or p53 ORF plus p53 5′ and 3′UTRs, were used as previously described [11]. GFP reporters that carry GFP-coding region alone, GFP plus p53 3′UTR, or GFP plus p53

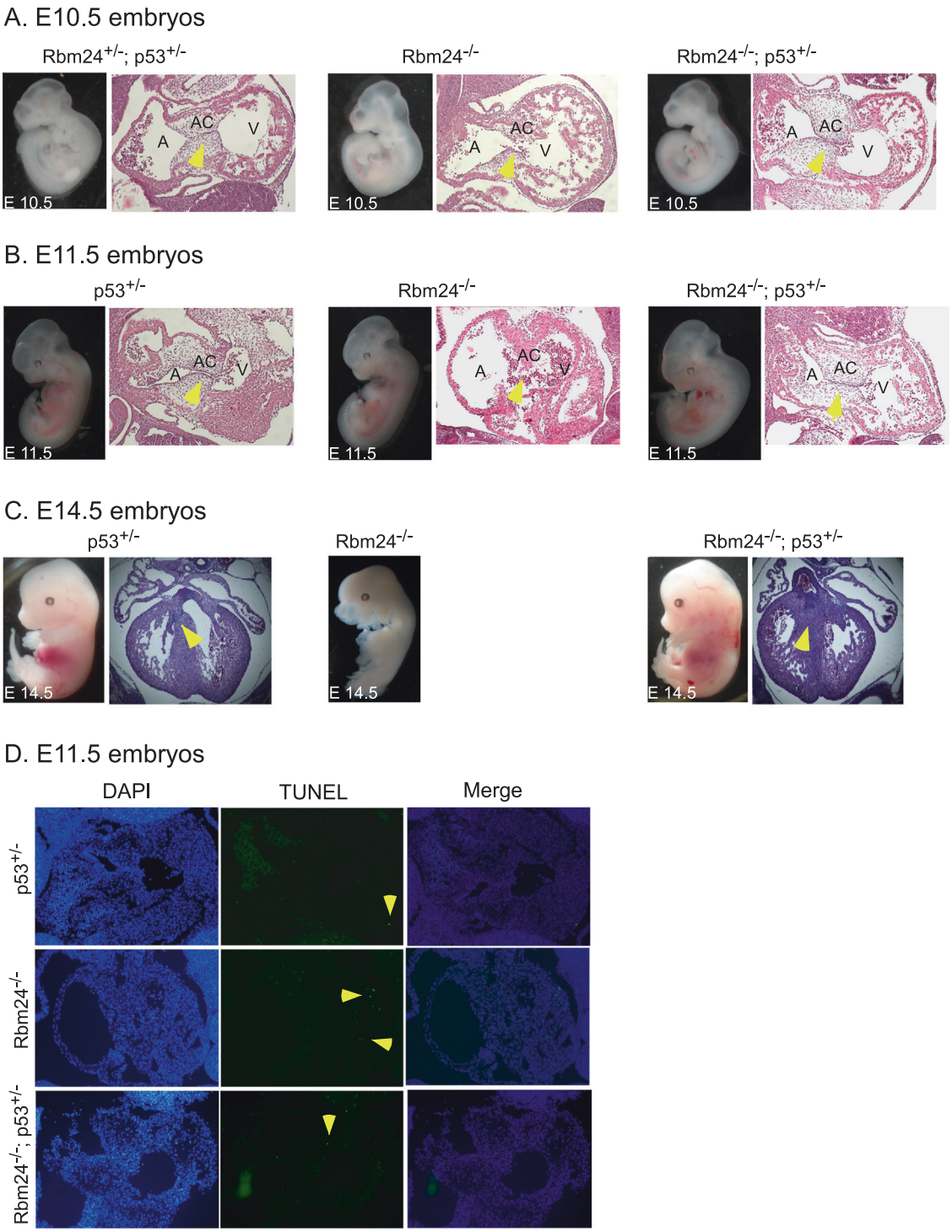


**Fig. 6** *Rbm24*$^{-/-}$ embryonic lethality and endocardial cushion defects are partially rescued by *p53* deficiency. **a–c** Representative images of E10.5 (**a**), E11.5 (**b**), and E14.5 (**c**) embryos and H&E-stained sagittal (**a**, **b**) or transverse (**c**) sections of heart with genotypes shown above the image. *A* atrium, *AC* atrioventicular cushion marked by yellow arrow, *V* ventricle. **d** TUNEL assay was performed with sagittal sections from *p53*$^{+/-}$, *Rbm24*$^{-/-}$, and *Rbm24*$^{-/-}$; *p53*$^{+/-}$ littermate embryos at E11.5. (Color figure online)

3′UTR with deletion of the poly (U)-rich region were used as previously described [43]. GST-tagged Rbm24 expression vector was used as previously described [7]. His-tagged eIF4E expression vector was used as previously described [11]. The pGL3 reporter that carries dual luciferases (Renilla Luc and Firefly Luc) and p53 5′UTR was generated using PCR. The primers for generating p53 5′ UTR are forward primer 5′-GGATCCTAATACGACTC ACTATAGGGAGGGAGCCTCGCAGGGGTTGAT-3′, and reverse primer, 5′-GGCAGTGACCCGGAAGGCA-3′.

### RNA isolation and RT-PCR

Total RNA was isolated with Trizol reagent. RT-PCR was performed with the Iscript cDNA synthesis kit (Bio-Rad Laboratories) according to the manufacturer's instructions. The primers used to amplify actin were forward primer 5′-CTGAAGTACCCCATCGAGCACGGCA-3′ and reverse primer 5′-GGATAGCACAGCCTGGATAGCAACG-3′. The primers used to amplify p53 were forward primer 5′-GACCGGCGCACAGAGGAAGAGAATC-3′ and reverse primer 5′-GAGTTTTTTATGGCGGGAGGTAGAC-3′. The primers used to amplify Rbm24 were forward primer 5′-AGCCTGCGCAAGTACTTCG-3′ and reverse primer 5′-CAGGCCCTTTCGGCAGCAG-3′.

### GST-pull down assay

Recombinant His-tagged and GST-tagged proteins were expressed in bacteria BL21 and purified by using Ni-NTA and glutathione sepharose beads, respectively. For GST-pull down assay, 500 ng of recombinant His-tagged proteins and 500 ng of recombinant GST-tagged proteins were incubated in E1A binding buffer (50 mM HEPES, pH 7.6, 50 mM NaCl, 5 mM EDTA, 0.1% Nonidet P-40, and 10% glycerol) for 1 h at 4 °C, followed by precipitation with glutathione-sepharose beads. After three washes, beads were re-suspended in 2× SDS loading buffer and subjected to western blot analysis.

### *Rbm24*-deficient and *p53*-deficient mice and primary MEFs

Conditional *Rbm24* knockout mice were generated by UC Davis Mouse Biology Program. Specifically, loxP sites were inserted in the *Rbm24* gene (Supplementary Fig. S1A). The resulting allele contains two loxP sites flanking exon 1 and exon 2. Mice with targeted allele were then bred with a cre deleter strain (Jackson Laboratories, stock no. 003314) expressing cre recombinase to delete exons 1–2. Mice were genotyped (Supplementary Fig. S1B) by PCR using primers as indicated in Supplementary Fig. S1A. For wild-type mice, a 245-bp fragment was detected using forward primer P1 (5′-CTAAGCAGAAGGGACGGTTC-3′) and reverse primer P2 (5′-GTGGGAGCCTTTGCACTC-3′). For *Rbm24* knockout mice, a 350-bp fragment was detected using forward primer P3 (5′-CTAGCTGTGAGCCATT AAAGC-3′) and reverse primer P4 (5′-CTTCCTA TGTGGCTGCTAGTAC-3′).

$p53^{+/-}$ mice (on C57BL/6 background) were purchased from the Jackson Laboratory. $Rbm24^{+/-}$ mice were crossed with $p53^{+/-}$ mice to generate double heterozygous mice. The latter were intercrossed to generate $Rbm24^{-/-}$; $p53^{+/-}$ and $Rbm24^{-/-}$; $p53^{-/-}$ mutant mice. All animals were housed at the University of California at Davis CLAS vivarium facility. The animal use protocols were approved by the University of California at Davis Institution Animal Care and Use Committee.

To generate MEFs, mice were bred and MEFs were isolated from 13.5-day-old embryos as described previously [44]. Primary MEFs were cultured in DMEM supplemented with 10% fetal bovine serum.

### Cell culture and cell line generation

H1299, RKO, MCF7, HCT116, and p53-null HCT116 were cultured in DMEM (Invitrogen) supplemented with 10% fetal bovine serum (Hyclone). The cell lines that inducibly express Rbm24 or HA-tagged Rbm24 were used and cultured as previously reported [7].

Rbm24 knockout cell lines were generated by CRISPR-cas9 genome editing method. sgRNAs targeting RBM24 were designed using the CRISPR design tool (http://tools.genome-engineering.org) and cloned into the BbsI sites of CRISPR vector pSpCas9(BB)-2A-Puro. Two specific gRNAs were used: gRNA #1 GTACACCAA-GATCTTCGTCG and gRNA #2 CGAGGTCTTCGGC-GAGATCG. The construct was transfected to MCF7, HCT116 and $p53^{-/-}$ HCT116 cells. Rbm24-KO cell lines were selected with puromycin and confirmed by sequence.

### Histology and TUNEL assay

Embryos at different stages of development were fixed in buffered formalin (pH 6.8–7.0) for 24 h and then stored in 70% ethanol. Tissues were paraffin-embedded and sectioned. Six-μm-thick sections were deparaffinized, rehydrated, and then stained with hematoxylin and eosin. TUNEL assay was performed with histological specimen fixed in formalin. TUNEL reaction mixture (Roche) was added to the surface of the sections and incubated for 1 h at 37 °C in a humidified atmosphere in the dark. All cells were counterstained with DAPI to visualize nuclei.

### RNA interference

Scramble siRNA (GGCCGAUUGUCAAAUAAUU), siRNA against human Rbm24 (CACUGGAGCUGCAU ACGCA) and siRNA against mouse Rbm24 (CACUG-GAGCCGCCUACGCU) were purchased from Dharmacon (Chicago, IL). For siRNA transfection, siLentFectTM Lipid Reagent (Bio-Rad) was used according to the user's manual. For lentiviral production, lentiviral vectors (pLKO.1-puro) expressing an shRNA of interest were purchased from Sigma. The targeting sequences are 5′-CGCTGAG-TACTTCGAAATGTC-3′ for control luciferase shRNA; 5′-GCGAGCAATATGTAGCTTGAA-3′ for Rbm24 shRNA#1; and 5′-CCCATCATTGATGGCA-GAAAG-3′ for Rbm24 shRNA#2. An shRNA-expression lentiviral vector (10 μg) along with packaging plasmids, pRSV-REV (5 μg), pMDL g/p RRE (5 μg), and VSVG (5 μg) were co-transfected into 293T cells ($1 \times 10^7$) by ExpressFectTM transfection system (Denville Scientific) according to the user's manual. After 48 h, the supernatant containing shRNA-expressing lentiviruses was filtered and concentrated by ultracentrifugation (28,000 r.p.m. for 1 h at 4 °C). The concentrated lentiviral particles were then trans-duced into cells, followed by puromycin selection (1 μg/ml) for 72 h.

### Western blot analysis and immunoprecipitation

Cell lysates suspended in 2× SDS sample buffer were resolved by SDS-PAGE, transferred to a nitrocellulose membrane, and probed with indicated antibodies. The immunoreactive bands were visualized by the enhanced chemiluminescence (Pierce) and quantified by densitometry with Software LabWorks (UVP, Upland, CA). Immunopre-cipitation assay was performed as previously described [45]. Briefly, cells were lysed in 0.2% Triton lysis buffer (25 mM Tris (pH 7.4), 25 mM NaCl, and 0.2% Triton X-100) sup-plemented with the proteinase inhibitor cocktail (100 μg/ml), followed by incubation with 1 μg of antibody or control IgG. The immunocomplexes were brought down by protein A/G beads and subjected to western blot analysis.

### $^{35}$S-metabolic labeling

The assay was performed as described [46]. Briefly, cells were preincubated in methionine-free DMEM for 1 h, and then labeled with 100 μCi/ml of $^{35}$S-methionine (Perki-nElmer) for 10 min. The incorporation of $^{35}$S-methionine into newly synthesized proteins was measured by TCA precipitation. Approximately $1 \times 10^7$ cpm of $^{35}$S-labeled lysates were immunoprecipitated with 1.0 μg of anti-p53. The immunocomplexes were resolved in SDS-PAGE gel and then subjected to autoradiography.

### RNA immunoprecipitation followed by RT-PCR analysis (RNA-ChIP)

RNA-chromatin immunoprecipitations (RNA-ChIP) was performed as described [47]. Cell extracts were prepared with immunoprecipitation buffer (100 mM KCl, 5 mM $MgCl_2$, 10 mM HEPEs, 1 mM 1,4-Dithiothreitol (DTT), and 0.5% NP-40) and then incubated with 2 μg of anti-HA, anti-eIF4E, or an isotype control IgG at 4 °C overnight. The RNA–protein immunocomplexes were brought down by protein A/G beads, followed by RT-PCR analysis.

### RNA electrophoretic mobility shift assay

p53 probes were created and RNA electrophoretic mobility shift assay (REMSA) were performed as described pre-viously [11] except that GST-RBM24 proteins were used.

### Polysome profile analysis

Polysome profile was performed as described [11]. Briefly, HCT116 cells were uninduced or induced to express Rbm24 for 24 h, treated with 0.1 mM cycloheximide for 30 min, and then lysed in a buffer containing 0.5% NP40, 0.1 M NaCl, 10 mM $MgCl_2$, 2 mM DTT, 50 mM Tris-HCl (pH 7.5), 200 U/mL SUPERase·In, 100 μg/mL cyclohex-imide, and 200 μg/mL heparin. Nuclei were precipitated at 10,000*g* for 10 min. The resulting supernatants were layered on a 15–45% (w/v) sucrose gradient containing 0.15 M NaCl, 5 mM $MgCl_2$, and 25 mM Tris-HCl (pH 7.5), and centrifuged in a SW40 rotor (Beckman Coulter) at 35,000 r. p.m. for 140 min. Gradients were analyzed by using ISCO fractionator with $UV_{254nm}$ detector, and RNAs were extracted from RNA–protein complexes with phenol–chloroform-isoamyl alcohol and recovered by ethanol precipitation. One microgram of total RNAs from each fraction was used for RT–PCR to detect p53 and actin transcripts. The primers to amplify p53 were 5′-CCCAGCCAAAGAAGAAACCA-3′ and 5′-GTTCCAAG GCCTCATTCAGCT-3′. The primers to amplify actin were 5′-CTGAAGTACCCCATCGAGCACGGCA-3′ and 5′-GGATAGCACAGCCTGGATAGCAACG-3′.

### Luciferase assay

A dual luciferase assay was performed in triplicate according to the manufacturer's instructions (Promega). Briefly, HCT116-RBM24$^{-/-}$ cells were plated at 50,000 cells/well in a 24-well plate and allowed to recover over-night. Cells were then co-transfected with 500 ng of pGL3 reporter vector (which contains firefly luciferase, Renilla luciferase, and p53 5′UTR) along with pcDNA3 or a pcDNA3 vector expressing Rbm24. Thirty-six hours post

transfection, luciferase activity was measured with the dual luciferase kit and Turner Designs luminometer. The fold increase in relative luciferase activity is a product of the luciferase activity induced by Rbm24 divided by that induced by empty pcDNA3 vector.

### Colony formation assay

Wild-type, Rbm24$^{-/-}$, p53$^{-/-}$, and p53$^{-/-}$;Rbm24$^{-/-}$ HCT116 cells (1000 per well) in six-well plates were cultured for 13–17 days. The clones were fixed with methanol/glacial acetic acid (7:1) and then stained with 0.1% of crystal violet [48].

**Acknowledgments** This work is supported in part by NIH grants CA076069.

**Authors' contribution** Zhang M., Zhang Y., Xu E., Mohibi S., Jiang Y., de Anda D.M., and Zhang J. did the experiments; Zhang M., Zhang Y., Zhang J., and Chen X. analyzed the data and wrote the manuscript. All authors read and approved the manuscript.

## Compliance with ethical standards

**Competing interest** The authors declare that they have no competing financial interest.

## References

1 Levine AJ, Oren M. The first 30 years ofp53: growing ever more complex. Nat Rev Cancer. 2009;9:749–58.
2 Vousden KH, Prives C. Blinded by the light: the growing complexity of p53. Cell. 2009;137:413–31.
3 Choi J, Donehower LA. p53 in embryonic development: maintaining a fine balance. Cell Mol Life Sci. 1999;55:38–47.
4 Grier JD, Xiong S, Elizondo-Fraire AC, Parant JM, Lozano G. Tissue-specific differences of p53 inhibition by Mdm2 and Mdm4. Mol Cell Biol. 2006;26:192–8.
5 Van Nostrand JL, Brady CA, Jung H, Fuentes DR, Kozak MM, Johnson TM, *et al* Inappropriate p53 activation during development induces features of CHARGE syndrome. Nature. 2014;514:228–32.
6 Zhang Q, He X, Chen L, Zhang C, Gao X, Yang Z, *et al* Synergistic regulation of p53 by Mdm2 and Mdm4 is critical in cardiac endocardial cushion morphogenesis during heart development. J Pathol. 2012;228:416–28.
7 Jiang Y, Zhang M, Qian Y, Xu E, Zhang J, Chen X. Rbm24, an RNA-binding protein and a target ofp53, regulates p21 expression via mRNA stability. J Biol Chem. 2014;289:3164–75.
8 Shu L, Yan W, Chen X. RNPC1, an RNA-binding protein and a target of the p53 family, is required for maintaining the stability of the basal and stress-induced p21 transcript. Genes Dev.2006;20:2961–72
9 Xu E, Zhang J, Zhang M, Jiang Y, Cho SJ, Chen X. RNA-binding protein RBM24 regulates p63 expression via mRNA stability. Mol Cancer Res. 2014;12:359–69.
10 Zhang J, Jun Cho S, Chen X. RNPC1, an RNA-binding protein and a target of the p53 family, regulates p63 expression through mRNA stability. Proc Natl Acad Sci USA.2010;107:9614–9
11 Zhang J, Cho SJ, Shu L, Yan W, Guerrero T, Kent M, *et al* Translational repression of p53 by RNPC1, a p53 target overexpressed in lymphomas. Genes Dev. 2011;25:1528–43.
12 Zhang J, Xu E, Ren C, Yan W, Zhang M, Chen M, *et al* Mice deficient in Rbm38, a target of the p53 family, are susceptible to accelerated aging and spontaneous tumors. Proc Natl Acad Sci USA. 2014;111:18637–42.
13 Poon KL, Tan KT, Wei YY, Ng CP, Colman A, Korzh V, *et al* RNA-binding protein RBM24 is required for sarcomere assembly and heart contractility. Cardiovasc Res. 2012;94:418–27.
14 Yang J, Hung LH, Licht T, Kostin S, Looso M, Khrameeva E, *et al* RBM24 is a major regulator of muscle-specific alternative splicing. Dev Cell. 2014;31:87–99.
15 Ray PS, Grover R, Das S. Two internal ribosome entry sites mediate the translation of p53 isoforms. EMBO Rep. 2006;7:404–10.
16 Vagner S, Galy B, Pyronnet S. Irresistible IRES. Attracting the translation machinery to internal ribosome entry sites. EMBO Rep. 2001;2:893–8.
17 Fisher SA, Langille BL, Srivastava D. Apoptosis during cardiovascular development. Circ Res. 2000;87:856–64.
18 Gaussin V, Van de Putte T, Mishina Y, Hanks MC, Zwijsen A, Huylebroeck D, *et al* Endocardial cushion and myocardial defects after cardiac myocyte-specific conditional deletion of the bone morphogenetic protein receptor ALK3. Proc Natl Acad Sci USA 2002;99:2878–83.
19 James TN. Apoptosis in congenital heart disease. Coron Artery Dis. 1997;8:599–616.
20 Poelmann RE, Gittenberger-de Groot AC. Apoptosis as an instrument in cardiovascular development. Birth Defects Res. 2005;75:305–13.
21 Liu P, Xu B, Cavalieri TA, Hock CE. Pifithrin-alpha attenuates p53-mediated apoptosis and improves cardiac function in response to myocardial ischemia/reperfusion in aged rats. Shock. 2006;26:608–14.
22 Liu Q, Wang G, Zhou G, Tan Y, Wang X, Wei W, *et al* Angiotensin II-induced p53-dependent cardiac apoptotic cell death: its prevention by metallothionein. Toxicol Lett. 2009;191:314–20.
23 Kang PM, Izumo S. Apoptosis and heart failure: a critical review of the literature. Circ Res. 2000;86:1107–13.
24 Kang PM, Izumo S. Apoptosis in heart failure: is there light at the end of the tunnel (TUNEL)? J Card Fail. 2000;6:43–46.
25 Jeffers JR, Parganas E, Lee Y, Yang C, Wang J, Brennan J, *et al* Puma is an essential mediator of p53-dependent and -independent apoptotic pathways. Cancer Cell. 2003;4:321–8.
26 Nakano K, Vousden KH. PUMA a novel proapoptotic gene, is induced by p53. Mol Cell. 2001;7:683–94.
27 Yu J, Zhang L, Hwang PM, Kinzler KW, Vogelstein B. PUMA induces the rapid apoptosis of colorectal cancer cells. Mol Cell. 2001;7:673–82.
28 Dor Y, Camenisch TD, Itin A, Fishman GI, McDonald JA, Carmeliet P, *et al* A novel role for VEGF in endocardial cushion formation and its potential contribution to congenital heart defects. Development. 2001;128:1531–8.
29 Birks EJ, Latif N, Enesa K, Folkvang T, Luong le A, Sarathchandra P, *et al* Elevated p53 expression is associated with dysregulation of the ubiquitin-proteasome system in dilated cardiomyopathy. Cardiovasc Res. 2008;79:472–80.
30 Gill C, Mestril R, Samali A. Losing heart: the role of apoptosis in heart disease--a novel therapeutic target? FASEB J. 2002;16:135–46.
31 Rezvani M, Barrans JD, Dai KS, Liew CC. Apoptosis-related genes expressed in cardiovascular development and disease: an EST approach. Cardiovasc Res. 2000;45:621–9.

32 Sano M, Minamino T, Toko H, Miyauchi H, Orimo M, Qin Y, *et al* p53-induced inhibition of Hif-1 causes cardiac dysfunction during pressure overload. Nature. 2007;446:444–8.
33 Tsipis A, Athanassiadou AM, Athanassiadou P, Kavantzas N, Agrogiannis G, Patsouris E. Apoptosis-related factorsp53, bcl-2 and the defects of force transmission in dilated cardiomyopathy. Pathol Res Pract. 2010;206:625–30.
34 Sajjad A, Novoyatleva T, Vergarajauregui S, Troidl C, Schermuly RT, Tucker HO, *et al* Lysine methyltransferase Smyd2 suppresses p53-dependent cardiomyocyte apoptosis. Biochim Biophys Acta. 2014;1843:2556–62.
35 Shukla PC, Singh KK, Quan A, Al-Omran M, Teoh H, Lovren F, *et al* BRCA1 is an essential regulator of heart function and survival following myocardial infarction. Nat Commun. 2011;2:593.
36 Xiong S, Van Pelt CS, Elizondo-Fraire AC, Fernandez-Garcia B, Lozano G. Loss of Mdm4 results in p53-dependent dilated cardiomyopathy. Circulation. 2007;115:2925–30.
37 Caprio C, Baldini A. p53 suppression partially rescues the mutant phenotype in mouse models of DiGeorge syndrome. Proc Natl Acad Sci USA. 2014;111:13385–90.
38 Altin SE, Schulze PC. p53-upregulated modulator of apoptosis (PUMA): a novel proapoptotic molecule in the failing heart. Circulation. 2011;124:7–8.
39 Li Y, Lv Z, Liu X, Su W, Wang C, Li N, *et al* Hypoxic postconditioning inhibits endoplasmic reticulum stress-mediated cardiomyocyte apoptosis by targeting PUMA. Shock. 2013;39:299–303.
40 Mandl A, Huong Pham L, Toth K, Zambetti G, Erhardt P. Puma deletion delays cardiac dysfunction in murine heart failure models through attenuation of apoptosis. Circulation. 2011; 124:31–39.
41 Nickson P, Toth A, Erhardt P. PUMA is critical for neonatal cardiomyocyte apoptosis induced by endoplasmic reticulum stress. Cardiovasc Res. 2007;73:48–56.
42 Toth A, Jeffers JR, Nickson P, Min JY, Morgan JP, Zambetti GP, *et al* Targeted deletion of Puma attenuates cardiomyocyte death and improves cardiac function during ischemia-reperfusion. Am J Physiol Heart Circ Physiol. 2006;291:H52–60.
43 Zhang, Y, Qian, Y, Zhang, J, Yan, W, Jung, YS, Chen, M et al. Ferredoxin reductase is critical for p53-dependent tumor suppression via iron regulatory protein 2. Genes Dev. 2017; 31: 1243-1256.
44 Scoumanne A, Cho SJ, Zhang J, Chen X. The cyclin-dependent kinase inhibitor p21 is regulated by RNA-binding protein PCBP4 via mRNA stability. Nucleic Acids Res. 2011;39: 213–24.
45 Zhang J, Chen X. DeltaNp73 modulates nerve growth factor-mediated neuronal differentiation through repression of TrkA. Mol Cell Biol. 2007;27:3868–80.
46 Bonifacino, JS Metabolic labeling with amino acids. Curr Protoc Protein Sci. 2001; Chapter 3: Unit 3 7.
47 Peritz T, Zeng F, Kannanayakal TJ, Kilk K, Eiriksdottir E, Langel U, *et al* Immunoprecipitation of mRNA-protein complexes. Nat Protoc. 2006;1:577–80.
48 Zhang M, Zhang J, Chen X, Cho SJ, Chen X. Glycogen synthase kinase 3 promotes p53 mRNA translation via phosphorylation of RNPC1. Genes Dev. 2013;27:2246–58.